Received: 31 January 2024 | Revised: 14 April 2024 | Accepted: 16 April 2024

DOI: 10.1002/wcms.1715

ADVANCED REVIEW

WIREs COMPUTATIONAL MOLECULAR SCIENCE WILEY

Time-resolved photoelectron spectroscopy via trajectory surface hopping

Pratip Chakraborty[1] | **Spiridoula Matsika**[2]

[1]Department of Chemistry, KTH Royal Institute of Technology, Stockholm, Sweden

[2]Department of Chemistry, Temple University, Philadelphia, Pennsylvania, USA

Correspondence
Spiridoula Matsika, Department of Chemistry, Temple University, Philadelphia, PA, 19122, USA.
Email: smatsika@temple.edu

Funding information
Basic Energy Sciences, Grant/Award Number: DE-FG02-08ER15983

Edited by: Sandra Luber, Associate Editor and Peter Schreiner, Editor-in-Chief

Abstract

Time-resolved photoelectron spectroscopy is a powerful pump-probe technique which can probe nonadiabatic dynamics in molecules. Interpretation of the experimental signals however requires input from theoretical simulations. Advances in electronic structure theory, nonadiabatic dynamics, and theory to calculate the ionization yields, have enabled accurate simulation of time-resolved photoelectron spectra leading to successful applications of the technique. We review the basic theory and steps involved in calculating time-resolved photoelectron spectra, and highlight successful applications.

This article is categorized under:

Electronic Structure Theory > Ab Initio Electronic Structure Methods

Theoretical and Physical Chemistry > Spectroscopy

KEYWORDS

excited states, ionization, nonadiabatic dynamics, pump-probe spectroscopy

1 | INTRODUCTION

The developments in femtosecond lasers and computational techniques have allowed for an expansion in the investigations of ultrafast excited state dynamics, providing a better understanding of photophysical and photochemical phenomena. These processes are important in organic photochemistry, biological processes, such as vision and photosynthesis, as well as, in energy conversion. Various pump-probe techniques have been developed to probe the excited state dynamics, such as time-resolved photoelectron spectroscopy, transient absorption, time-resolved x-ray absorption, ultrafast electron diffraction, and others.[1–10] Time-resolved photoelectron spectroscopy (TRPES) is one of the most widely used techniques to study excited state dynamics and the nonadiabatic events involved.[1–6] Figure 1 from an early review by Stolow[3] illustrates how it can be used to provide information about nonadiabatic transitions between different electronic states. After a pump pulse excites the molecules, a probe pulse ionizes from the excited state and the created photoelectron is detected as a function of pump-probe delay. Assuming that the ionization probabilities and ionization energies are different for different electronic states, the appearance and disappearance of features in the photoelectron spectrum can provide information about the transition time scales. This picture is based on the idea that in some cases the electronically excited states ionize into different electronic continua based on their character, and this correlation allows for the simultaneous monitoring of both electronic and vibrational excited state dynamics. In practice, time-resolved photoelectron spectra are rarely so easily assigned as the cartoon in Figure 1 suggests, so their interpretation requires additional information from theoretical calculations.

Theoretical chemistry for excited states has also made great progress in the last decade.[11] Many electronic structure methods have been developed or became more efficient for studying excited states. The most appropriate and

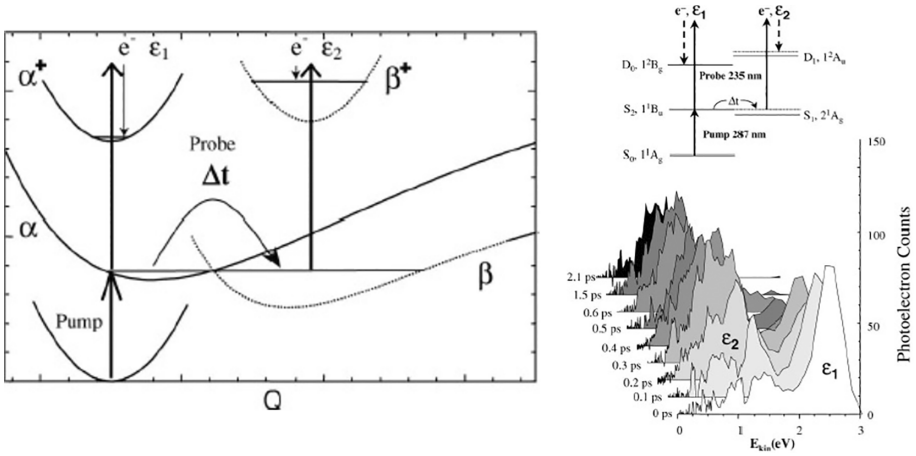

FIGURE 1 (Left) A TRPES scheme for disentangling electronic from vibrational dynamics in excited polyatomic molecules. An electronic state α is prepared by a fs pump pulse. Via a nonadiabatic process, it converts to a vibrationally hot lower lying electronic state, β. Based on the Koopmans'-type ionization correlations, if these two states ionize into different electronic continua, this will allow for the simultaneous monitoring of both electronic and vibrational excited state dynamics. (Right, Top) Energy level scheme for TRPES of all-trans decatetraene. The pump laser prepares the optically bright state S_2. Upon ultrafast internal conversion, this state converts to the lower lying state S_1 with >0.7 eV of vibrational energy. (Right, Bottom) TRPES spectra of this molecule pumped at 287 nm and probed at 235 nm. Figures used with permission from Annual Reviews, Inc, from Ref [3]; permission conveyed through Copyright Clearance Center, Inc.

traditional way to treat nonadiabatic processes is by using multireference methods.[12] Analytic gradients and nonadiabatic couplings have been developed and implemented for most multireference methods making them available for dynamics. Alternative more efficient methods are also being developed which can be used in nonadiabatic problems.[13–15] Nonadiabatic dynamics have also become more available. In particular on-the-fly dynamics, such as trajectory surface hopping (TSH),[16] ab initio multiple spawning,[17] variational multi-configurational Gaussian (vMCG) approach,[18] have enabled application to a great variety of polyatomic molecular systems which would be very hard or impossible to study using wavepacket dynamics.

For many studies of nonadiabatic processes, the comparison between theory and experiment has been qualitative, where the excited state lifetimes obtained by fitting the experimental signal have been compared to the theoretical population decays from the nonadiabatic dynamics.[19] This, however, can be problematic, since it completely ignores the probe and any effect it can have on the signal.[20] Figure 2 shows a previous theoretical study that demonstrated that neglecting the effect of the probe in ethylene leads to longer lifetimes, while incorporating it by modeling the photoelectron signal provides good agreement with experiment (due to widowing effects). So, the most appropriate way to make a satisfactory comparison between theory and experiment is to calculate the experimental observable. In most recent years, theory has moved into this stage, where the observable can be calculated after the propagation of the excited state dynamics. In addition to TRPES, there are several other observables that have been calculated, such as two-dimensional electronic spectra, stimulated emission, x-ray absorption and photoscattering, transient absorption, and ultrafast electron diffraction signals.[21–26]

In this review we will discuss the theoretical steps that are involved into calculating a TRPES, and provide some examples on the useful insight that can be obtained by comparing directly to experimental TRPES.

2 | THEORY

2.1 | General theory for simulating time-resolved photoelectron spectra

Theoretical approaches to calculate femtosecond TRPES were initially developed in the 1990s, primarily using analytic potentials on small systems, quantum wavepackets to describe the excited states, and electronic scattering continua for the photoionization.[27–31] While these studies provide a more rigorous theory for TRPES, they are challenging to apply to large polyatomic molecules, so semiclassical approaches have become more useful. Semiclassical formulations for TRPES which can be combined with TSH have been developed.[32–40] Bonačić-Koutecký, Mitric, and coworkers

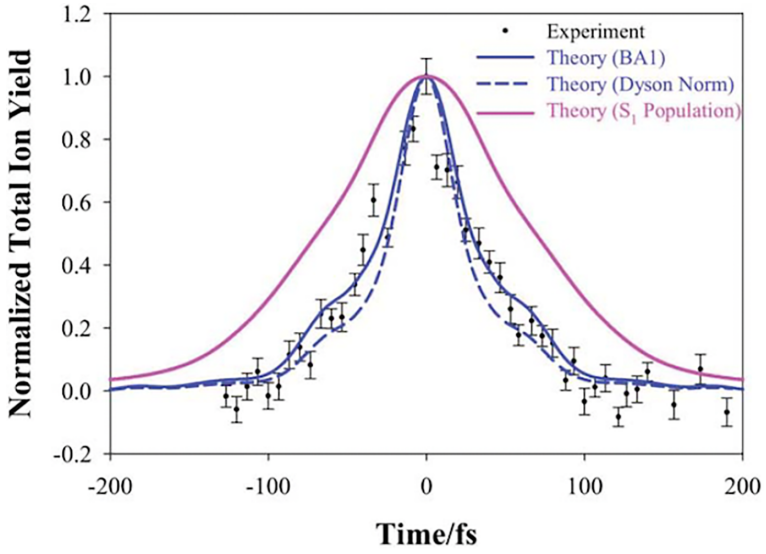

FIGURE 2 Comparison between experimental total ion yield and ab initio multiple spawning with multistate perturbation theory (AIMS-MSPT2) predicted signals. Experimental signal is shown as black dots with error bars. The calculated signals (from integrating the AIMS-MSPT2 predicted single photon TRPES spectra over all photoelectron energies) are shown in blue lines. The solid blue line is the first-order Born approximation (BA1) method (where the photoelectron wavefunction is approximated with a spherical wave) and the dashed blue line is the Dyson-Norm method. The pink line shows the photoion yield that would result from assuming that all S_1 population is ionizable (corresponding to using the population from the dynamics). This assumption leads to much slower decay of the photoion signal compared to the experiment. Reprinted from Ref. [20], with the permission of AIP Publishing.

pioneered the trajectory description of TRPES signals using the initial ideas of the Liouville space theory of pump-probe spectroscopy in the density matrix representation developed by Mukamel and coworkers[41] and a Wigner distribution approach, while incorporating many improvements.[32–38] Bennett et al.[23] have shown that a Fermi Golden Rule expression for the photoionization can be obtained as a limiting case of a more general theory. The limiting case semiclassical approach we present here based on this Fermi Golden Rule expression is valid for weak intensity of the ionizing radiation so that multiple ionization is avoided and the perturbation theory limit is valid. The pump and probe pulses are also approximated as non-overlapping, and any effect of the pulses on the signal is neglected. In addition, interactions between the photoelectron and the remaining cation are neglected. The photoionization time is very fast compared to the nuclear dynamics, so the Condon approximation is used, and the ionization is implied fast and vertical, i.e., the nuclear wave functions of the initial and final states are identical. The purpose of this work is to present how TRPES has been calculated using TSH in the most common approaches in the literature, which has been using these approximations. Readers interested in the underlying theory, its limitations, and ways to improve, are referred to the original publications.[23,32]

The photoelectron signal is calculated as the transition probability for photoionization where the scattering states of the electron are not taken into account. This signal associated with a specific photoionization frequency ω, $S(t,\epsilon_k,\omega)$, electron kinetic energy ϵ_k at time t, can be written as

$$S(t,\epsilon_k,\omega) = \sum_{F}^{ion.states} \int d\boldsymbol{R}\rho_I^t(\boldsymbol{R}(t))\sigma_{IF}(\boldsymbol{R}(t),\epsilon_k,\omega) \times \delta(\hbar\omega - \Delta V_{IF}(\boldsymbol{R}(t)) - \Delta K_{IF}(\boldsymbol{R}(t)) - \epsilon_k) \quad (1)$$

Ionization occurs from an initial state I, with an initial ensemble distribution of nuclear coordinates $\boldsymbol{R}$ (t) at time t, $\rho_I^t(\boldsymbol{R}(t))$, to a sum of final states F. σ_{IF} is the cross section for ionization given below, $\Delta V_{IF} = V_F - V_I$ is the difference of the vertical electronic energies of the initial neutral (I) and final ionic (F) states (vertical ionization potential), and ϵ_k is the kinetic energy of the ejected electron. $\hbar\omega$ is the probe photon energy. We assume that the electron ejection event is ultrafast. Therefore, the transition is fully vertical, so the nuclear kinetic/vibrational energy of the initial and final states are identical (i.e., $\Delta K_{IF} = 0$).

Using semiclassical trajectories generated from nonadiabatic dynamics simulations, we obtain the distribution ρ_I^t at a given time t, and the integral becomes a sum over $l = 1...N_p$ nuclear geometries obtained from trajectories, $\boldsymbol{R}_l(t)$. The photoelectron signal for time step t is given by

$$S(t,\epsilon_k,\omega) = \sum_{F}^{ion.states} \frac{1}{N_p} \sum_{l}^{N_p} \sigma_{IF}(\boldsymbol{R}_l(t),\epsilon_k,\omega)\delta(\hbar\omega - \Delta V_{IF}(\boldsymbol{R}_l(t)) - \epsilon_k) \tag{2}$$

The δ function represents the conservation of energy, where the energy of the photon is used to ionize the molecule and the remaining is kinetic energy of the photoelectron. However, since we are using discrete trajectory ensemble, a line shape function W is required. A normalized Gaussian or Lorentzian is often used centered at $\hbar\omega - \Delta V_{IF}(t)$ with a finite width which is a parameter. The function W however can also take a different form to take into account the fact that the kinetic energy between initial and final state is not realistically the same, that is, $\Delta K_{IF} \neq 0$. An alternative W that has been used[35,40,42] is a step function which is 0 for $\epsilon_k > \hbar\omega - \Delta V_{IF}(t)$ and 1 for $\epsilon_k \leq \hbar\omega - \Delta V_{IF}(t)$. This function assumes that all the available kinetic energies of the ionized state are possible and the photoelectron can have any energy between 0 and the maximum value of $\hbar\omega - \Delta V_{IF}(t)$. ΔV_{IF} and σ_{IF} depend on the geometry obtained at each time step during the trajectories, $\boldsymbol{R}_l(t)$.

Finally, we need a way to calculate the cross section σ_{IF}. Within the dipole approximation the cross section is proportional to the square of the electric dipole transition moment

$$\sigma_{IF} \propto \left| \left\langle \Psi_I | \boldsymbol{\mu} \cdot \boldsymbol{\varepsilon} | \Phi_F^k \right\rangle \right|^2 \tag{3}$$

Here $\boldsymbol{\mu} \cdot \boldsymbol{\varepsilon}$ is the scalar product of the dipole operator and the laser electric field. Ψ_I is the wavefunction of the initial N electron state, Φ_F^k is the wavefunction of the final state which includes the photoelectron with momentum k. If we express Φ_F^k as an antisymmetric product of the $(N-1)$ Ψ_F wavefunction and the photoelectron χ^k wavefunction, the dipole transition moment can be simplified

$$\left\langle \Psi_I | \boldsymbol{\mu} \cdot \boldsymbol{\varepsilon} | \Psi_F \chi^k \right\rangle = \left\langle \psi_{IF}^d | \boldsymbol{\mu} \cdot \boldsymbol{\varepsilon} | \chi^k \right\rangle \tag{4}$$

ψ_{IF}^d is the Dyson orbital which is defined as the overlap between the initial N electron electronic state (Ψ_I) and the final $N-1$ electron state (Ψ_F),

$$\psi_{IF}^d = \sqrt{N} \int \Psi_I(x_1, x_2, ...x_N)^* \Psi_F(x_1, x_2, ...x_{N-1}) dx_1 dx_2 ... dx_{N-1}. \tag{5}$$

Assuming photoelectron ejection is fast, an approximation is invoked that the state of the $N-1$ system does not interact with the outgoing electron. Because the treatment of the continuum is difficult, the most common approach has been to approximate the wave function of the ejected electron using plane or Coulomb waves.[20,37,38,43–45] The ezDyson software[45,46] is a freely available software that uses plane waves or Coulomb waves to describe the continuum state of the photoelectron. It calculates absolute photodetachment/photoionization cross sections, photoelectron angular distributions (PADs), and anisotropy parameters (β) using Dyson orbitals computed by an ab initio program. Even in that case several approximations remain including the neglect of the interaction of the outgoing electron with the core.[43,44] More sophisticated descriptions of the continuum are possible.[47–49] For example, the Schrödinger equation for the photoelectron wave function can be solved at the static-exchange density functional theory (DFT) level using a multicenter B-spline basis. This approach has been integrated with TSH to obtain TRPES.[47,49]

An additional approximation is to completely neglect the wavefunction of the ejected electron and approximate the intensity with the square of the Dyson norm. This approximation is actually the most commonly used approach in the literature and several studies have shown that it has a small effect on the photoelectron spectrum.[20,40,42] Comparisons between the Dyson norms and a more complete calculation of the ionization intensities have been made. Figure 3 shows a comparison between Dyson norms for both ionization from the ground state and from an excited state using the time-dependent resolution in ionic states (TD-RIS) approach.[51] This approach includes the continuum

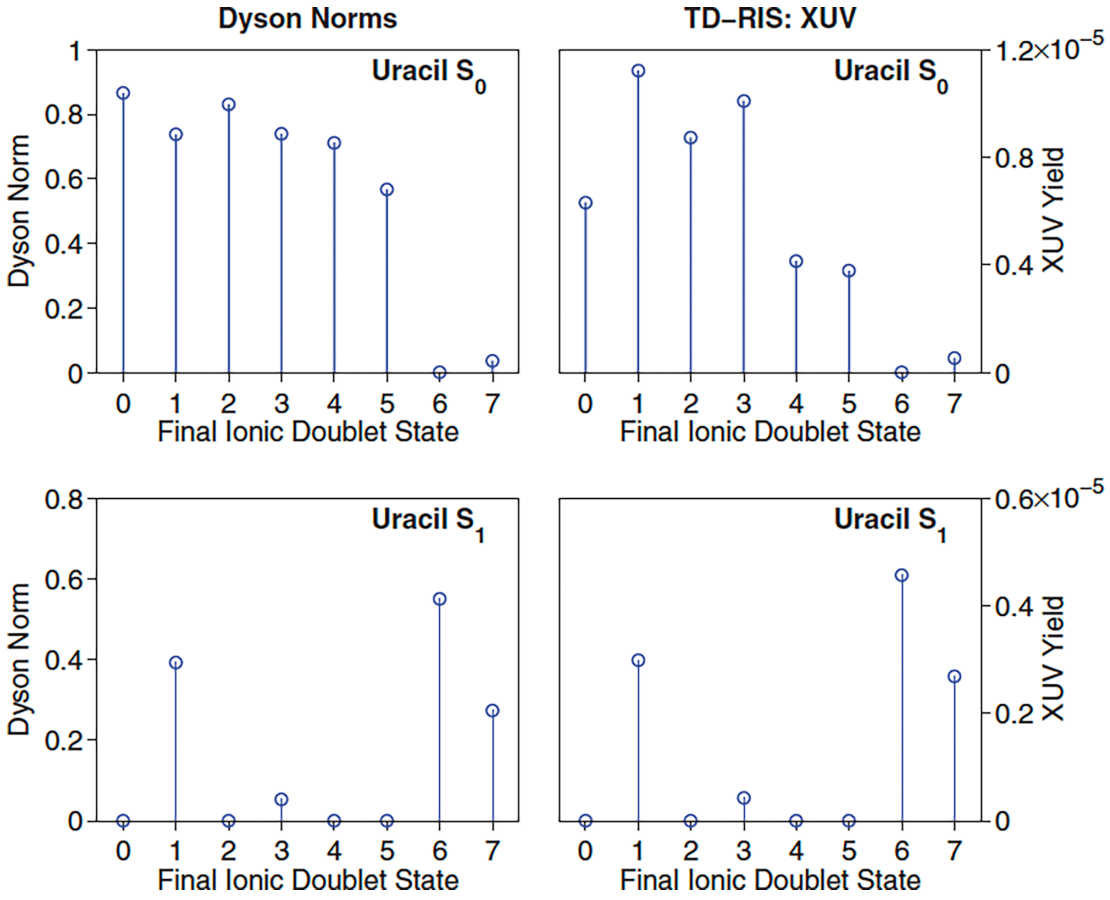

FIGURE 3 Comparison of the Dyson norms (left) with the time-dependent resolution in ionic states (TD-RIS) XUV ionization yields (right) for ionization from the lowest two singlet states of uracil (top, S_0; bottom, S_1). Reprinted figure with permission from Ref. [50]. Copyright 2012 by the American Physical Society.

wavefunction of the ejected electron and the coupling with the ion remaining behind. The approximations used are that the continuum electron is not antisymmetrized with the remaining bound electrons upon ionization, and only a finite number of cationic states are included. It is clear from the figure that the Dyson norms provide a very good description of the ionization intensities, particularly from the excited state. Figure 2 also shows a comparison between the integrated photoelectron spectrum obtained using the Dyson norms or including the wavefunction of the ejected electron. It is again clear that the two spectra are very similar. Angular distributions of photoelectrons, however, require a more detailed description of the continuum function beyond the Dyson norms. It should also be noted that there are cases where the transition dipole is energy dependent even at low energies, such as photodetachment in anions. Moreover, the transition dipole for different electronic channels may be different. Nevertheless, neglecting the electron continuum functions seems to be appropriate for the case studies discussed here.

We will now discuss how to calculate the different parts that go into the calculation of the TRPES signal as depicted in Equation (2). Here we focus on TSH to obtain the N_p sampling combined with different electronic structure methods to obtain the energies and Dyson norms. We will not discuss angular distributions and asymmetry parameters, but rather focus on the simpler approaches where only the Dyson norms are used.

2.2 | Electronic structure methods

The first and very important step in being able to reproduce TRPES is the choice of electronic structure method. The electronic structure method should be able to accurately describe energies, forces and nonadiabatic couplings of excited states along the relevant potential energy surfaces (PES) visited during the dynamics. At the same time, in order to calculate the signal, we need to be able to accurately calculate the ionization energies along the dynamical pathways, and

the Dyson norms between the neutral and ionic states which provide the intensities. This provides many constrains on finding the appropriate methods, but luckily it is not always necessary to choose the same method for the dynamics and the calculation of the signal. It is possible to run the nonadiabatic dynamics first with a particular method and then the produced geometries can be used to calculate the ionization energies and intensities (with a different method) that will be used to reproduce the spectrum. This may be necessary since the methods that can be reliable for excited states may not be as good for ionic states. There are, however, limitations to this approach, and it has to be used very carefully. It is important that the different methods predict similar excited state PES. If they do not, for example, if they predict different ordering of states, or different shapes of the surfaces leading to conical intersections at different places, the results will be erroneous. We will briefly discuss the possible electronic structure choices here and advantages and disadvantages.

A detailed review of electronic structure methods suitable for nonadiabatic dynamics and conical intersections can be found in a recent publication.[52] Traditionally, multireference methods offer the best choice for nonadiabatic dynamics since they can treat multiple electronic states on equal footing, which is essential for these dynamics.[53,54] Most of the dynamics studies and modeling of TRPES have been done using multireference methods. Complete Active Space Self Consistent Field (CASSCF) is the most common choice since it is not as computationally intense as multirerefence methods that include dynamical correlation. CASSCF includes only nondynamical correlation and usually provides a qualitatively correct description of excited states and dynamics, but in many cases it fails to give a quantitatively accurate description. Dynamical correlation can be included either using perturbation theory on a multireference zeroth order description, and several variations have been developed (CASPT2, NEVPT2, MCQDPT2, etc.) or by using multireference configuration interaction (MRCI) which is based on varational principle.[53,54] CASPT2 should be used in a multistate variant (XMS-CASPT2 or XDW-CASPT2 or RMS-CASPT2) since state specific corrections can be very problematic near conical intersections and avoided crossings.[55–57] TRPES modeling has actually been used to test the importance of dynamical correlation in reproducing the dynamics.[58,59]

Multireference methods, however, are computationally intensive, even at the CASSCF level. So many efforts have been made to develop alternatives. Single reference methods can be used to treat couplings between excited states, but they cannot treat coupling with the ground state in their basic forms. TDDFT is a very widely used approach and has been used in dynamics and in modeling of TRPES.[33,35,60] Other methods, such as ADC(2) and CC2,[61,62] have been used for nonadiabatic dynamics, and ADC(2) has also been used as the underlying dynamics method to calculate TRPES.[49] This is definitely not an exhaustive list of methods used for nonadiabatic dynamics, but we focus more on methods that have been used in combination with TRPES modeling.

Appropriate electronic structure methods are also needed for the ionization energies and the Dyson norms. The most natural approach would be to use the same approach for the neutral states and their dynamics as well as the TRPES signal. This has commonly been done with CASSCF. CASSCF has the advantage that it can include all the states of interest for both the neutral and the cation, and it can provide a reliable description on regions of conical intersections with the ground state. The ionization potentials (IPs), however, are not very accurate because of the imbalance of correlation between neutral and cation. So the calculated TRPES may need to be shifted in order to be compared with experiment. A CASSCF calculation of the neutral and one for the cation is needed at every time step and the difference of energies provides the IPs. Dyson orbitals and their norms can be calculated by the overlap of the wavefunctions. CASPT2 for both dynamics and ionization signals has also been used.[63]

In a different approach, the ionization energies and Dyson orbitals can be obtained with a different method than the dynamics. In this case, it is very important to match the excited states calculated by the method used in TSH and the method used in the Dyson norms. An approach that seems reasonable is to combine a multireference method for TSH with equation of motion for ionization potentials coupled cluster with singles and doubles (EOM-IP-CCSD), since EOM-IP-CCSD is a much better approach to calculate accurate IPs. The computational software QChem[64] is able to calculate IP from excited states and the corresponding Dyson orbitals. Caution is needed, however, since certain states may not be available with this approach. Figure 4 shows an example where the excited and ionic states are calculated with EOM-CCSD (EOM-EE-CCSD for neutral and EOM-IP-CCSD for cation) vs XMS-CASPT2. The EOM-IP-CCSD gives good energies for the IPs, but it completely omits an ionic state that is parallel to the neutral excited state, because this state involves rearrangement of the electrons after electron ejection. At the EOM-IP-CCSD level, all cation states are destabilized along the path towards the conical intersection. At the CASPT2 level, however, D_4 is initially stabilized, the energy is lowered starting from the Franck Condon region. As a consequence, it crosses D_3 and the lower states. Diabatically, this state is parallel to the neutral S_1 state, and the resulting photoelectron spectrum will have constant kinetic energy along this reaction coordinate, creating a photoelectron signal that is constant as a function of time. This

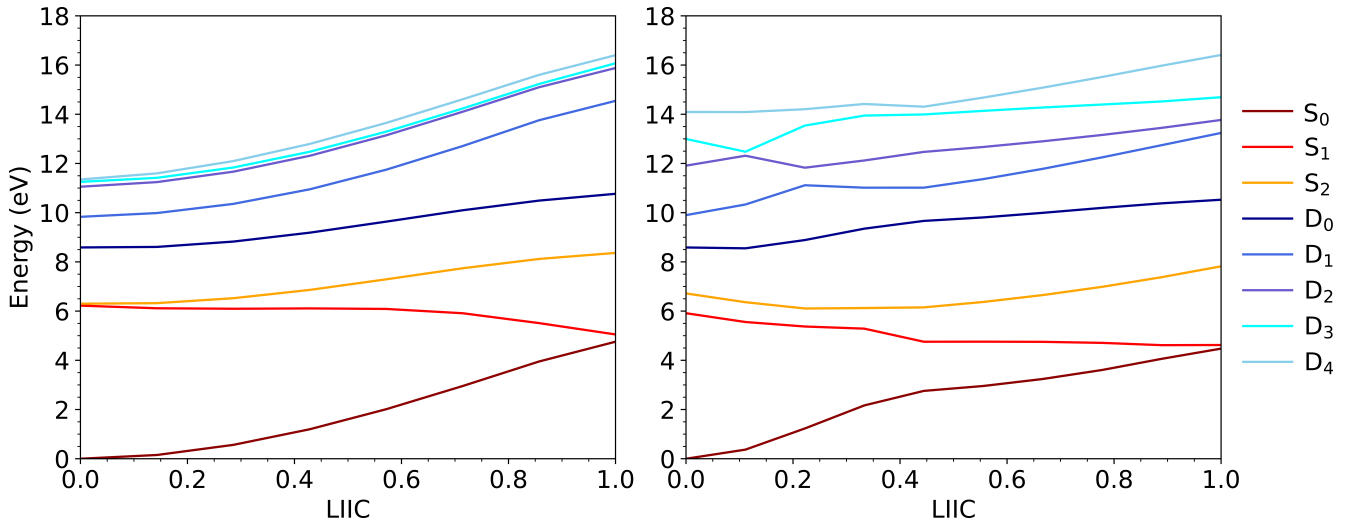

FIGURE 4 Energies of neutral (S_0, S_1, S_2) and ionic (D_0, ...D_4) states of 1,3-cis,cis-cyclooctadiene calculated with EOM-EE-CCSD/EOM-IP-CCSD (left) and XMS-CASPT2/CAS(5/6,6)/cc-pVDZ (right) along a linearly interpolated path from the Franck-Condon geometry to a conical intersection. The x-axis is dimensionless.

can only be generated using the multireference methods for the cation. At the EOM-IP-CCSD level, any photoelectron signal generated will decrease kinetic energy as a function of time, and it does not reproduce the experimental signals. So this state is essential for reproducing the TRPES. Overall, careful testing has to be done if a mixing of methods is used.

2.3 | Initial conditions

Semiclassical trajectory surface hopping has emerged as a popular method to study excited state dynamics in polyatomic molecules. The first step in this approach involves sampling of initial conditions. Initial conditions are also necessary for simulating static spectra and providing the broadening of the spectra. The ensemble of initial geometries represents the vibrational distribution of the ground initial state. There are two common ways to obtain the ensemble, either by dynamics on the ground state (which can use classical force fields or ab initio forces) or by using a Wigner distribution.[65] For condensed phase systems, ground state dynamics is the most common way to obtain the nuclear ensemble, and that takes into account thermal distributions and anharmonicity but cannot account for zero point energy. On the other hand, the Wigner distribution takes into account the zero point energy and is most often used for isolated molecular systems. For small-to-medium sized molecules, the Wigner distribution of the harmonic oscillator is the most common approach. The effect of the different ensemble approaches on the spectra and dynamics have been discussed before in the literature.[66,67] Recently, quantum thermostatting (QT), which thermalizes the normal modes of a molecule at their individual frequency-dependent temperatures using the Generalized Langevin Equation (GLE) thermostat,[68,69] has also been employed as an alternative to Wigner sampling to illustrate that such a sampling is preferable when low-frequency anharmonic vibrational modes are present.[70]

In a static spectrum these geometries are used to calculate the signal. In time-resolved spectroscopy the geometries are used as initial conditions to start the dynamics on the excited states. In pump-probe spectroscopies, however, one also has to consider that the initial pump excitation occurs using a laser pulse with a particular wavelength and time resolution, so it does not usually excite the whole spectrum. A proper way to take this into account would be to incorporate the pump pulse in the dynamics. But this usually is not done since it is time consuming and the absorption cross section is small. Alternatively, a vertical instantaneous excitation is assumed and only the nuclear configurations whose vertical excitation corresponds to the laser frequency plus or minus an energy window are used. An illustration of this approach is shown in Figure 5 which shows the gas phase absorption spectrum of uracil, calculated with various electronic structure methods and superimposed to the experimental spectrum.[58] The absorption spectra calculated by a Wigner distribution reproduce well the shape of the experimental spectrum in this case although the absorption maximum is predicted to be shifted (in most cases blue-shifted) depending on the accuracy of the electronic structure

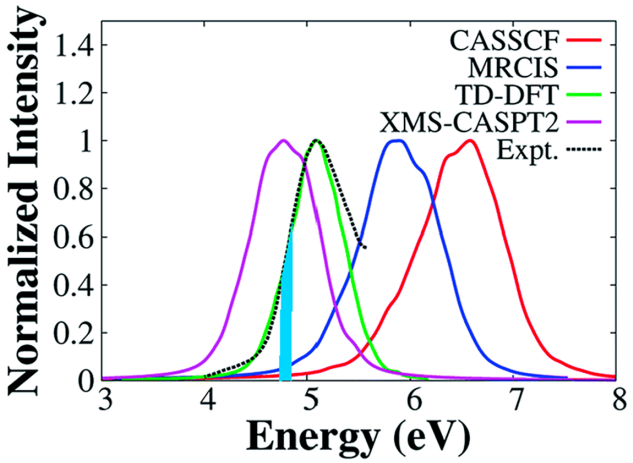

FIGURE 5 Normalized absorption spectrum (first absorption band) of uracil at CASSCF, MRCIS, XMS-CASPT2 and TDDFT levels overlayed with the experimental first absorption band taken from Ref. [71]. The thick vertical cyan line centered at 4.8 eV represents the excitation pulse. Reproduced from Ref. [58] with permission from the Royal Society of Chemistry.

method used. The pulse laser used in the TRPES experiment excited the molecule at 260 nm (=4.77 eV), so in our study to reproduce this, theoretically, we first shifted the calculated spectra to the experimental maximum and then only picked configurations within the window of 4.77 ± 0.15 eV.[58]

2.4 | Trajectory surface hopping methodology

In order to simulate the time-resolved photoelectron spectral signal, nonadiabatic excited state dynamics need to be performed. The most popular method to tackle nonadiabatic dynamics is to employ the TSH dynamics.[72–76] In TSH, the electronic degrees of freedom are treated quantum mechanically, whereas the nuclear degrees of freedom are treated classically. In this method, the time evolution of a wavepacket is approximated as a swarm of independent classical nuclear trajectories sampling different regions of the multi-dimensional PES. Energies, gradients/forces and nonadiabatic couplings are calculated using quantum chemical methods at every time step of the classical trajectories on-the-fly, along with transition probabilities of hopping from one electronic state to another. The classical trajectories are propagated on these PESs, generated on-the-fly, using Newton's equation of motion, whereas the electronic coefficients are propagated using the time-dependent Schrödinger equation. Such a method totally avoids prior construction of the multi-dimensional PES, which is one of the most important advantages of TSH with respect to quantum dynamics methods. Also, for small-to-medium sized systems, all nuclear degrees of freedom can be explored in TSH unlike quantum dynamics. In TSH, each classical trajectory, at any time, is only propagated on one Born-Oppenheimer electronic state, and Tully's fewest switches surface hopping (FSSH) method[77] is commonly employed along with a stochastic algorithm, that allows for hopping between electronic states, to simulate the splitting of the wavepacket due to nonadiabatic effects.

The intuitive formalism, on-the-fly PES generation along with the full nuclear dimensional treatment, allows TSH to be more practical and computationally less expensive compared to wavepacket propagation and other quantum dynamics methods such as multi-configurational time-dependent Hartree (MCTDH).[78] However, the approximations involved in the formalism lead to certain issues. Tunneling cannot be treated via TSH because of the inherent local character of the method. In order to reach statistical convergence, a large number of trajectories are required to be propagated. Moreover, if ab initio electronic structure methods are employed to construct the full dimensional on-the-fly PESs, it makes the procedure often computationally demanding. Thus, TSH simulations are, currently, computationally tractable up to only a few picoseconds for real systems. Nonetheless, recently, there has been a lot of development in predicting on-the-fly PESs for trajectory propagation using machine learning based techniques.[79–82] This is promising since it opens up the possibility for propagating significantly more trajectories for longer timescale.[83]

Another problem with the original TSH formalism is that it does not capture decoherence (or loss of coherence) between the electronic states. A quantum wavepacket can split into multiple components while evolving through a

strong nonadiabatic coupling region. These newly spawned components evolving on their respective electronic states, are coupled to each other, initially. However, as they propagate away from the strong coupling region, following different gradients on different electronic states, the coherence between them is lost, progressively. In TSH, the electronic wavefunction is propagated in a fully coherent manner. Thus, several decoherence corrections have been developed to approximately capture decoherence.[84–92] The most popular and computationally cheap method to include decoherence is to use an empirical parameter based correction scheme in the framework of mean field methods[84,85] called the non-linear decay of mixing approach, which was adopted by Granucci and Persico,[86] in TSH. Here, a decoherence time is defined based on the energy difference of the states involved, classical kinetic energy of the nuclei, and two empirical parameters. The aforementioned decohence time is used to correct the electronic coefficients non-linearly at every time step after integration of the electronic Schrödinger equation, which maintains the internal consistency in the populations. Decoherence corrections can also be derived in a more rigorous way from the exact factorization approach when that approach is used in a surface hopping scheme.[93,94]

An extension of TSH has also been developed for simulating nonadiabatic dynamics called surface hopping including arbitrary couplings (SHARC).[73,95,96] As the name suggests, such a technique allows for simulating nonadiabatic dynamics of molecules that can include any type of couplings such as nonadiabatic coupling, spin-orbit coupling, dipole moment-laser field couplings, in equal footing. In SHARC method, the Hamiltonian consisting of these couplings is diagonalized in order to propagate classical trajectories on the PESs incorporating the effect of all the couplings, thus permitting the treatment of processes beyond internal conversion, such as intersystem crossing and laser-induced excitation.

Currently, there exist several codes which can perform some flavor of TSH for molecular systems (interfaced to electronic structure codes), including Newton-X,[97,98] SHARC,[96,99] JADE,[100] PYXAID,[101] Libra[102] and ANT.[103]

Another technique that has been employed to propagate nonadiabatic dynamics, and simulate TRPES based on such dynamics, is called ab-initio multiple spawning (AIMS).[17,104] AIMS is an intermediate between full quantum dynamics such as wavepacket propagation, and mixed quantum-classical methods, like TSH. In AIMS, the time-dependent nuclear wave function corresponding to each electronic state is expanded as a linear combination of multi-dimensional, frozen Gaussian basis functions, termed trajectory basis functions (TBF), with complex time-dependent coefficients. The multi-dimensional PES and nonadiabatic couplings are calculated on-the-fly similar to TSH, and the TBFs are propagated on those PESs. Unlike TSH, the splitting of the wavepacket in strong nonadiabatic coupling region is approximated by allowing spawning of new TBFs. As such, this method also provides an improved description of decoherence between the electronic states. However, this method can also be computationally demanding as new spawning events around strong nonadiabatic coupling regions lead to an increase in the number of TBFs requiring an ever-increasing number of electronic structure calculations at later time steps. There are several other mixed-quantum classical and full quantum dynamics methods to treat nonadiabatic dynamics, which can be utilized to calculate TRPES. References [16, 17] provide descriptive review of such techniques.

2.5 | Dyson norms

After nonadiabatic dynamics, the second step is to calculate the ionization energies and Dyson norms at every time step. In some of the earlier studies, the Dyson norms were not calculated and intensities were assumed to be constant.[33,35] This may be appropriate for static photoelectron spectra where ionization occurs from the ground state and the probability to remove an electron from a given orbital is not very different for different orbitals. But, when ionizing from an excited state, the probabilities can be very different. Koopmans' theorem provides a simple illustration of that. Koopmans' theorem assumes a single Slater determinant description of the initial or final state and neglects any orbital relaxation after ionization, i.e. the same orbitals are used to build both the neutral and the cation Slater determinants and only the occupancies are different. In this approximation, the ionization energy to remove an electron is equal to the negative of the orbital energy, while the overlap between the neutral and cationic wavefunctions is the orbital describing the hole left behind after the electron is removed. Figure 6 shows an illustration of how Koopmans' theorem can be used to understand ionization probabilities before Dyson norms are calculated. This example is a direct demonstration of the correlations discussed in Figure 1. If an excited state is described by a HOMO → LUMO excitation, ionization is most likely to occur by removal of an electron from the HOMO or LUMO orbitals leading to ionic states D_0 and D_3 in the figure. But reaching a cationic state with a hole in the HOMO-1 orbital and a configuration $(\text{HOMO-1})^1(\text{HOMO})^2$ (state D_1) will not be allowed based on Koopmans' theorem, since it requires rearrangement of

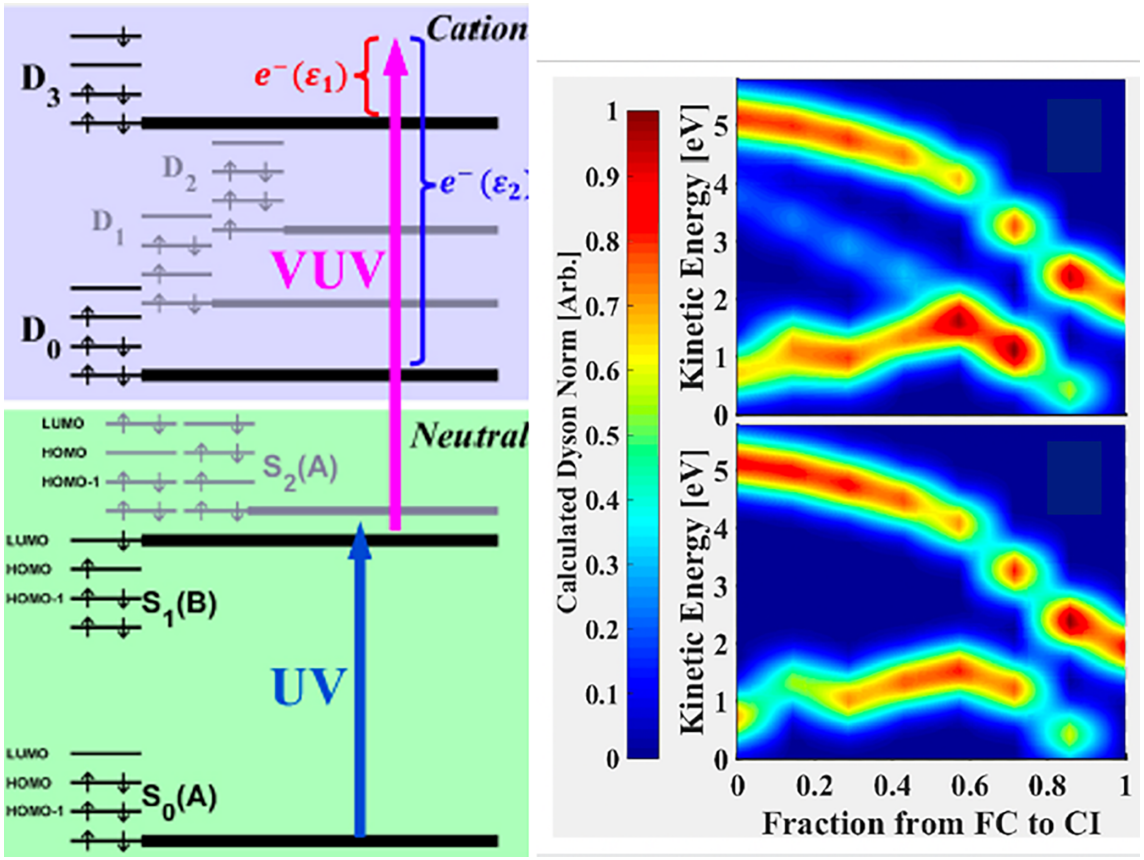

FIGURE 6 (Left) A cartoon depiction of low lying neutral and cationic states, electron orbital occupancies, and Koopmans' correlations in the pump–probe measurements of 1,3-cis,cis-cyclooctadiene (COD). Three neutral and four cationic states are included. The UV pump pulse excites the molecule to a singly excited bright state, S_1(B), in which an electron in the highest occupied molecular orbital (HOMO) is promoted to the lowest unoccupied molecular orbital (LUMO). Ionization to the two cationic states favored by Koopmans' correlations (D_3 and D_0) is illustrated by the pink arrow, producing photoelectrons with energies ϵ_1 and ϵ_2, respectively. (Right) (top) Calculated Dyson norm values between S_1 and all the cationic states. (bottom) Dyson norm values only from S_1 to D_0 and D_3. The x axis represents a linear interpolation coordinate connecting the Franck-Condon geometry of COD to a conical intersection between S_1 and S_0. Reprinted from Ref. [105], with the permission of AIP Publishing.

multiple electrons. Even though Koopmans' theorem is very simple and can be applied without any calculation of Dyson norms, it provides a good first order approximation to the selection rules, or ionization probabilities. The right panel of Figure 6 shows photoelectron signals calculated using Dyson norms or just Koopman probabilities (1 or 0) and the results are very similar qualitatively.

Nevertheless, this is not always the case. The importance of Dyson orbitals has been highlighted,[106,107] and they have been calculated using several electronic-structure methods, such as TDDFT[37,38,40] CASSCF,[108–111] CASPT2,[49] and CCSD.[43–45,47] Requirements of the electronic structure to obtain accurate Dyson norms and angular distributions have also been explored.[112]

3 | APPLICATIONS

In this section, we will summarize and highlight recent studies where TRPES signals have been calculated and compared to experiments. This is not intended to be an exhaustive list, but we want to highlight the progress in the field. First studies of employing TSH to simulate TRPES appeared in 2007 applied to cytosine using CASSCF[108] and anionic gold clusters using TDDFT.[33] Other studies by Bonačić-Koutecký, Mitric, and coworkers also used TDDFT and TSH applied to several other molecules.[32–38] Other groups have also used TDDFT with TSH. For example, cyclohexadiene

has been studied with this approach and compared to an experimental TRPES using 267 nm pump and 400 nm probe.[60]

TRPES has been calculated using AIMS on many systems.[63,108,113–120] Important insight was provided by these studies for nucleobases, butadiene and its substituted derivatives and other organic systems. Most of these studies have compared their calculated spectra to experimental TRPES by Stolow and coworkers. One and two photon ionization has been used in the experiments using tuneable femtosecond UV laser pulses.

Barbatti and coworkers have incorporated the calculation of TRPES in the NewtonX[98] TSH code and demonstrated its use on imidazole.[40] TRPES for several molecules has been modeled using TSH by the group of Gonzalez using their SHARC software[96] for the TSH. The advantage of their approach is that they can include spin-orbit coupling into the simulations making it the preferred choice for systems where intersystem crossing is important. Nucleobases and thionucleobases have been studied.[42,121] In 2018 thiouracil, a molecule where intersystem crossing is important, was studied in collaboration with Susanne Ullrich's group who performed TRPES using 293 nm excitation and 194 nm one-photon ionization.[42] Pitesa et al. have also used TSH to predict TRPES, and in their work they included the ejected electron wavefunction so they were able to predict angular distributions as well for pyrazine.[49]

Our group has simulated TRPES spectra for several systems in collaboration with the experimental group of Weinacht.[58,59,105,111,122,123] In the experiment, the excitation is facilitated by an ultrashort UV pulse which is the third harmonic (260 nm) of the fundamental (IR centered at 780 nm) of a Ti:sapphire laser, while the ionizing probe occurs through a time-delayed vacuum-UV (VUV) probe pulse with a central wavelength around 156 nm (7.9 eV).

As an illustration of the approach, we will show results for uracil. Experimental TRPES was obtained by Weinacht and coworkers and our group simulated the TRPES using multireference methods, CASSCF, MRCIS, and XMS-CASPT2, all with the active space of 12 electrons in 9 orbitals (12,9) and the cc-pVDZ basis set. The details of this study have been discussed in Ref. [58,59] The absorption spectra of uracil obtained using a Wigner distribution of a harmonic oscillator for the ground state are shown in Figure 5 together with the pump pulse centered at 4.77 eV. Initial conditions were obtained using geometries that contributed to the absorption at 4.77 ± 0.15 eV. Because the spectra obtained with the theoretical methods were shifted compared to the experimental spectrum, the corresponding shift was used in choosing geometries, so geometries for CASSCF and XMS-CASPT2 for example were obtained at 6.29 ± 0.15 eV, and 4.49 ± 0.15 eV, respectively. TSH was run using these geometries and TRPES was calculated along the dynamics using CASSCF Dyson norms. In the MRCIS and XMS-CASPT2 studies, the character of the states had to be checked so that the appropriate Dyson norms were calculated when using CASSCF. The resulting TRPES from CASSCF and XMS-CASPT2 are shown in Figure 7 and compared with experiment. The two-dimensional spectrum is shown on the left, while the signal has been integrated over photoelectron energies on the right side. It is obvious from the comparisons with the experimental spectrum that CASSCF cannot reproduce the experimental signal while XMS-CASPT2 does a much better job, especially for the higher energy part of the spectrum. This study highlighted the importance of dynamical correlation in understanding the excited state dynamics in uracil, an important biomolecule, and it predicted that the decay from the bright S_2 state is very fast, less than 100 fs.

4 | CONCLUSION

Advances in methods for electronic structure theory, nonadiabatic dynamics, and ionization cross sections, have enabled accurate simulations of time-resolved photoelectron spectroscopy. Several studies have been published in the last decade taking advantage of these advances and calculating TRPES in order to interpret the experimental spectra and reveal the underlying molecular dynamics. Through these studies, it has become evident that the best approach to learn more about the dynamics of molecules is through combined studies where theory and experiment work together, and direct comparisons of the same observables are being made.

While great advances have been made, there is still need for improvements in all aspects of the calculations. Electronic structure methods for excited states and nonadiabatic events, including conical intersections and dissociation, are still not efficient enough to be applied to large molecules. There is a lot of methodological developments in this area, and we expect the methods to continue improving in accuracy and efficiency. Similarly, trajectory surface hopping has extended the applicability of excited state dynamics, but it has several deficiencies that are being addressed by the community. Finally, calculating the ionization cross sections can also be improved beyond Dyson norms. All these challenges offer opportunities for development. It is encouraging however that even at the current stage, we are able to calculate spectra that agree very well with experiment for molecules of up to 10–20 atoms.

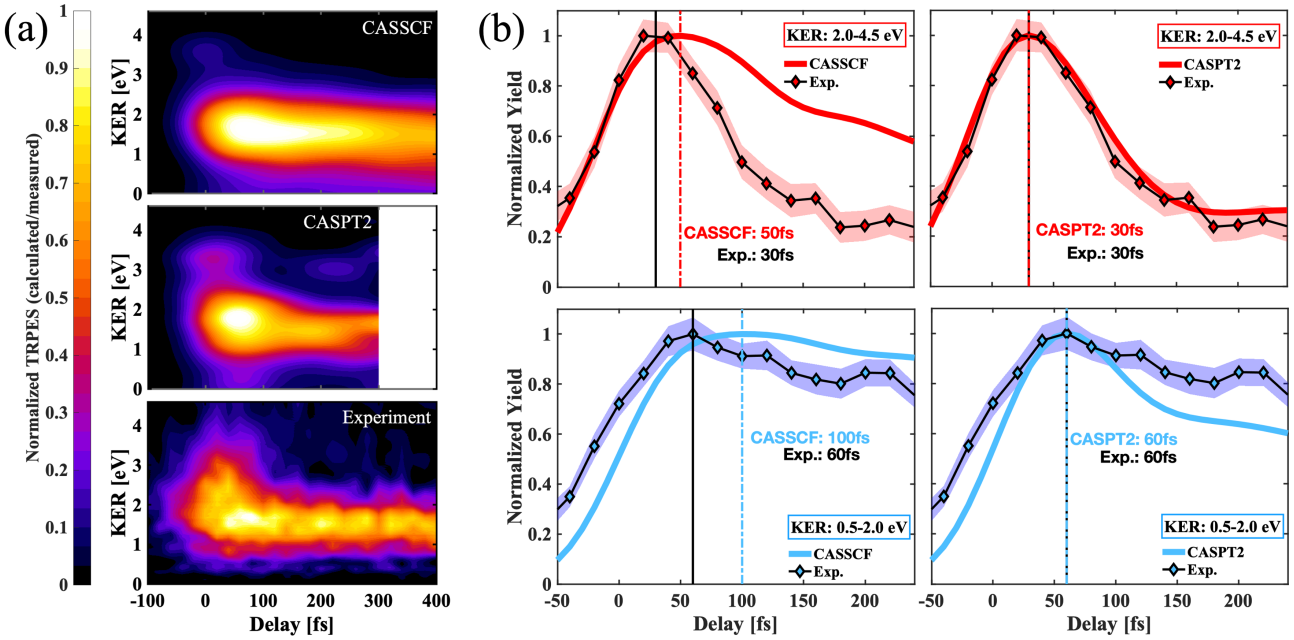

FIGURE 7 Time-dependent photoelectron yield of uracil. (a) TRPES obtained from simulations (CASSCF and XMS-CASPT2) and experimental spectrum. (b) TRPES integrated over two different energy ranges. Panels in the top show measured and simulated yields for electrons between 2.0 and 4.5 eV. Panels in the bottom show measured and simulated yields for the lower energy range covered between 0.5 and 2.0 eV. The two columns in (b) show the calculated yields from trajectories propagated at the CASSCF (left two panels) and XMS-CASPT2 (right two panels) levels. In each panel, the vertical black line indicates the peak locations for the higher and lower energy ranges of the measured TRPES. Reprinted with permission from Ref. [123] Copyright 2022 American Chemical Society.

AUTHOR CONTRIBUTIONS

Pratip Chakraborty: Data curation (equal); formal analysis (equal); investigation (equal); methodology (equal); validation (equal); visualization (equal); writing – original draft (equal); writing – review and editing (equal). **Spiridoula Matsika:** Conceptualization (equal); funding acquisition (equal); project administration (equal); supervision (equal); writing – original draft (equal); writing – review and editing (equal).

FUNDING INFORMATION

This work was supported by the US Department of Energy (award: DE-FG02-08ER15983).

CONFLICT OF INTEREST STATEMENT

The authors declare no conflicts of interest.

DATA AVAILABILITY STATEMENT

Data sharing is not applicable to this article as no new data were created or analyzed in this study.

ORCID

Pratip Chakraborty https://orcid.org/0000-0002-0248-6193
Spiridoula Matsika https://orcid.org/0000-0003-2773-3979

RELATED WIREs ARTICLES

Newton-X: A surface-hopping program for nonadiabatic molecular dynamics
The ezSpectra suite: An easy-to-use toolkit for spectroscopy modeling
Columbus-a program system for advanced multireference theory calculations

REFERENCES

1. Blanchet V, Zgierski MZ, Seideman T, Stolow A. Discerning vibronic molecular dynamics using time-resolved photoelectron spectroscopy. Nature. 1999;401(6748):52–4.
2. Neumark DM. Time-resolved photoelectron spectroscopy of molecules and clusters. Annu Rev Phys Chem. 2003;54:89–119.
3. Stolow A. Femtosecond time-resolved photoelectron spectroscopy of polyatomic molecules. Annu Rev Phys Chem. 2003;54:89–119.
4. Stolow A, Bragg AE, Neumark DM. Femtosecond time-resolved photoelectron spectroscopy. Chem Rev. 2004;104(4):1719–58.
5. Suzuki T. Femtosecond time-resolved photoelectron imaging. Annu Rev Phys Chem. 2006;57:555–92.
6. Suzuki T. Time-resolved photoelectron spectroscopy of non-adiabatic electronic dynamics in gas and liquid phases. Int Rev Phys Chem. 2012;31(2):265–318.
7. Kochman MA, Durbeej B, Kubas A. Simulation and analysis of the transient absorption Spectrum of 4-(N,N-Dimethylamino)benzonitrile (DMABN) in acetonitrile. J Phys Chem A. 2021;125(39):8635–48. https://doi.org/10.1021/acs.jpca.1c06166
8. Avagliano D, Bonfanti M, Nenov A, Garavelli M. Automatized protocol and interface to simulate QM/MM time-resolved transient absorption at TD-DFT level with COBRAMM. J Comput Chem. 2022;43(24):1641–55. https://doi.org/10.1002/jcc.26966
9. Hohenstein EG, Yu JK, Bannwarth C, List NH, Paul AC, Folkestad SD, et al. Predictions of pre-edge features in time-resolved near-edge X-ray absorption fine structure spectroscopy from hole–hole Tamm–Dancoff-approximated density functional theory. J Chem Theory Comput. 2021;17(11):7120–33. https://doi.org/10.1021/acs.jctc.1c00478
10. Centurion M, Wolf TJA, Yang J. Ultrafast imaging of molecules with electron diffraction. Annu Rev Phys Chem. 2022;73(1):21–42. https://doi.org/10.1146/annurev-physchem-082720-010539
11. Matsika S, Krylov AI. Introduction: theoretical modeling of excited state processes. Chem Rev. 2018;118:6925–6.
12. Lischka H, Nachtigallová D, Aquino AJA, Szalay PG, Plasser F, Machado FBC, et al. Multireference approaches for excited states of molecules. Chem Rev. 2018;118(15):7293–361. https://doi.org/10.1021/acs.chemrev.8b00244
13. Gagliardi L, Truhlar DG, Li Manni G, Carlson RK, Hoyer CE, Bao JL. Multiconfiguration pair-density functional theory: a new way to treat strongly correlated systems. Acc Chem Res. 2017;50(1):66–73. https://doi.org/10.1021/acs.accounts.6b00471
14. Hollas D, Šištík L, Hohenstein EG, Martínez TJ, Slavíček P. Nonadiabatic ab initio molecular dynamics with the floating occupation molecular orbital-complete active space configuration interaction method. J Chem Theory Comput. 2018;14(1):339–50. https://doi.org/10.1021/acs.jctc.7b00958
15. de Wergifosse M, Grimme S. Perspective on simplified quantum chemistry methods for excited states and response properties. J Phys Chem A. 2021;125:3841–51.
16. Crespo-Otero R, Barbatti M. Recent advances and perspectives on nonadiabatic mixed quantum–classical dynamics. Chem Rev. 2018;118(15):7026–68.
17. Curchod BF, Martínez TJ. Ab initio nonadiabatic quantum molecular dynamics. Chem Rev. 2018;118(7):3305–36.
18. Worth GA, Lasorne B. 13. In: gaussian wave packets and the DD-vMCG approach. Chichester, West Sussex: John Wiley Sons, Ltd; 2020. p. 413–33. https://doi.org/10.1002/9781119417774.ch13
19. Fielding HH, Worth GA. Using time-resolved photoelectron spectroscopy to unravel the electronic relaxation dynamics of photoexcited molecules. Chem Soc Rev. 2018;47:309–21.
20. Tao H, Allison T, Wright T, Stooke A, Khurmi C, van Tilborg J, et al. Ultrafast internal conversion in ethylene. I. The excited state lifetime. J Chem Phys. 2011;134(24):244306.
21. Polli D, Altoe P, Weingart O, Spillane KM, Manzoni C, Brida D, et al. Conical intersection dynamics of the primary photoisomerization event in vision. Nature. 2010;467:440–3. https://doi.org/10.1038/nature09346
22. Rivalta I, Nenov A, Cerullo G, Mukamel S, Garavelli M. Ab initio simulations of two-dimensional electronic spectra: the SOS// QM/-MM approach. Int J Quantum Chem. 2014;114:85–93.
23. Bennett K, Kowalewski M, Mukamel S. Probing electronic and vibrational dynamics in molecules by time-resolved photoelectron, auger-electron, and X-ray photon scattering spectroscopy. Faraday Discuss. 2015;177:405–28.
24. Tenorio BNC, Pedersen J, Barbatti M, Decleva P, Coriani S. Auger–Meitner and x-ray absorption spectra of ethylene cation: insight into conical intersection dynamics. J Phys Chem A. 2024;128:107–17.
25. Wolf WJA, Sanchez DM, Yang J, Parrish RM, Nunes JPF, Centurion M, et al. The photochemical ring-opening of 1,3-cyclohexadiene imaged by ultrafast electron diffraction. Nat Chem. 2019;11:504–9.
26. Silfies MC, Mehmood A, Kowzan G, Hohenstein EG, Levine BG, Allison TK. Ultrafast internal conversion and photochromism in gas-phase salicylideneaniline. J Chem Phys. 2023;159:104304. https://doi.org/10.1063/5.0161238
27. Seel M, Domcke W. Femtosecond time-resolved ionization spectroscopy of ultrafast internal-conversion dynamics in polyatomic molecules: theory and computational studies. J Chem Phys. 1991;95:7806–22.
28. Meier C, Engel V. Mapping of wave-packet dynamics in a double-well potential via femtosecond pump-probe photoelectron spectroscopy. J Chem Phys. 1994;101:2673–7.
29. Seideman T. Time-resolved photoelectron angular distributions: a nonperturbative theory. J Chem Phys. 1997;107:7859–68.
30. Arasaki Y, Takatsuka K, Wang K, McKoy V. Femtosecond energy- and angle-resolved photoelectron spectroscopy. J Chem Phys. 2000;112:8871–84.
31. Batista VS, Zanni MT, Greenblatt BJ, Neumark DM, Miller WH. Femtosecond photoelectron spectroscopy of the I_2^- molecular dynamics simulation method. J Chem Phys. 1999;110:3736.

32. Bonačić-Koutecký V, Mitrić R. Theoretical exploration of ultrafast dynamics in atomic clusters: analysis and control. Chem Rev. 2005; 105:11–65.
33. Stanzel J, Burmeister F, Neeb M, Eberhardt W, Mitrić R, Bürgel C, et al. Size-dependent dynamics in excited states of gold clusters: from oscillatory motion to photoinduced melting. J Chem Phys. 2007;127:164312.
34. Mitrić R, Werner U, Bonačić-Koutecký V. Nonadiabatic dynamics and simulation of time resolved photoelectron spectra within time-dependent density functional theory: ultrafast photoswitching in benzylideneaniline. J Chem Phys. 2008;129:164118.
35. Fuji T, Suzuki YI, Horio T, Suzuki T, Mitrić R, Werner U, et al. Ultrafast photodynamics of furan. J Chem Phys. 2010;133(23):234303. https://doi.org/10.1063/1.3518441
36. Werner U, Mitrić R, Bonačić-Koutecký V. Simulation of time resolved photoelectron spectra with Stieltjes imaging illustrated on ultrafast internal conversion in pyrazine. J Chem Phys. 2010;132:174301. https://doi.org/10.1063/1.3395160
37. Humeniuk A, Wohlgemuth M, Suzuki T, Mitrić R. Time-resolved photoelectron imaging spectra from non-adiabatic molecular dynamics simulations. J Chem Phys. 2013;139:134104.
38. Tomasello G, Humeniuk A, Mitrić R. Exploring ultrafast dynamics of pyrazine by timeresolved photoelectron imaging. J Phys Chem A. 2014;118:8437–45.
39. Ren H, Fingerhut BP, Mukamel S. Time resolved photoelectron spectroscopy of thioflavin T photoisomerization: a simulation study. J Phys Chem A. 2013;117(29):6096–104. https://doi.org/10.1021/jp400044t
40. Arbelo-González W, Crespo-Otero R, Barbatti M. Steady and time-resolved photoelectron spectra based on nuclear ensembles. J Chem Theory Comput. 2016;12:5037–49.
41. Yan YJ, Fried LE, Mukamel S. Ultrafast pump-probe spectroscopy: femtosecond dynamics in Liouville space. J Phys Chem. 1989;93: 8149–62.
42. Mai S, Mohamadzade A, Marquetand P, González L, Ullrich S. Simulated and experimental time-resolved photoelectron spectra of the intersystem crossing dynamics in 2-thiouracil. Molecules. 2018;23(11):2836.
43. Oana CM, Krylov AI. Dyson orbitals for ionization from the ground and electronically excited states within equation-of-motion coupled-cluster formalism: theory, implementation, and examples. J Chem Phys. 2007;127:234106.
44. Oana CM, Krylov AI. Cross sections and photoelectron angular distributions in photodetachment from negative ions using equation-of-motion coupled-cluster Dyson orbitals. J Chem Phys. 2009;131:124114.
45. Gozem S, Gunina AO, Ichino T, Osborn DL, Stanton JF, Krylov AI. Photoelectron wave function in photoionization: plane wave or coulomb wave? J Phys Chem Lett. 2015;6:4532–40.
46. Gozem S, Krylov AI. The ezSpectra suite: an easy-to-use toolkit for spectroscopy modeling. WIREs Comput Mol Sci. 2022;12:e1546.
47. Moitra T, Ponzi A, Koch H, Coriani S, Decleva P. On the accurate description of photoionization dynamical parameters. J Phys Chem Lett. 2020;11:5330–7.
48. Ponzi A, Sapunar M, Angeli C, Cimiraglia R, Došlić N, Decleva P. Photoionization of furan from the ground and excited electronic states. J Chem Phys. 2016;144:084307.
49. Piteša T, Sapunar M, Ponzi A, Gelin MF, Došlić N, Domcke W, et al. Combined surface- hopping, Dyson orbital, and B-spline approach for the computation of time-resolved photoelectron spectroscopy signals: the internal conversion in pyrazine. J Chem Theory Comput. 2021;17(8):5098–109. https://doi.org/10.1021/acs.jctc.1c00396
50. Spanner M, Patchkovskii S, Zhou C, Matsika S, Kotur M, Weinacht TC. Dyson norms in XUV and strong-field ionization of polyatomics: cytosine and uracil. Phys Rev A. 2012;86:053406.
51. Spanner M, Patchkovskii S. One-electron ionization of multielectron systems in strong nonresonant laser fields. Phys Rev A. 2009;80: 063411.
52. Matsika S. Electronic structure methods for the description of nonadiabatic effects and conical intersections. Chem Rev. 2021;121: 9407–49.
53. Lischka H, Nachtigallova D, Aquino AJA, Szalay PG, Plasser F, Machado FBC, et al. Multireference approaches for excited states of molecules. Chem Rev. 2018;118:7293–361.
54. Park JW, Al-Saadon R, MacLeod MK, Shiozaki T, Vlaisavljevich B. Multireference electron correlation methods: journeys along potential energy surfaces. Chem Rev. 2020;120:5878–909.
55. Shiozaki T, Győrffy W, Celani P, Werner HJ. Communication: extended multi-state complete active space second-order perturbation theory: energy and nuclear gradients. J Chem Phys. 2011;135(8):081106. https://doi.org/10.1063/1.3633329
56. Battaglia S, Lindh R. Extended dynamically weighted CASPT2: the best of two worlds. J Chem Theory Comput. 2020;16(3):1555–67. https://doi.org/10.1021/acs.jctc.9b01129
57. Nishimoto Y, Battaglia S, Lindh R. Analytic first-order derivatives of (X)MS, XDW, and RMS variants of the CASPT2 and RASPT2 methods. J Chem Theory Comput. 2022;18(7):4269–81. https://doi.org/10.1021/acs.jctc.2c00301
58. Chakraborty P, Liu Y, Weinacht T, Matsika S. Effect of dynamic correlation on the ultrafast relaxation of uracil in the gas phase. Faraday Discuss. 2021;228:266–85. https://doi.org/10.1039/D0FD00110D
59. Chakraborty P, Liu Y, McClung S, Weinacht T, Matsika S. Time resolved photoelectron spectroscopy as a test of electronic structure and nonadiabatic dynamics. J Phys Chem Lett. 2021;12:5099–104.
60. Schalk O, Geng T, Thompson T, Baluyot N, Thomas RD, Tapavicza E, et al. Cyclohexadiene revisited: a time-resolved photoelectron spectroscopy and ab initio study. J Phys Chem A. 2016;120(15):2320–9.

61. Lischka H, Barbatti M, Siddique F, Das A, Aquino AJA. The effect of hydrogen bonding on the nonadiabatic dynamics of a thymine-water cluster. Chem Phys. 2018;515:472–9.
62. Plasser F, Crespo-Otero R, Pederzoli M, Pittner J, Lischka H, Barbatti M. Surface hopping dynamics with correlated single-reference methods: 9H-adenine as a case study. J Chem Theory Comput. 2014;10(4):1395–405.
63. Glover WJ, Mori T, Schuurman MS, Boguslavskiy AE, Schalk O, Stolow A, et al. Excited state non-adiabatic dynamics of the smallest polyene, trans 1, 3-butadiene. II. Ab initio multiple spawning simulations. J Chem Phys. 2018;148(16):164303.
64. Shao Y, Gan Z, Epifanovsky E, Gilbert ATB, Wormit M, Kussmann J, et al. Advances in molecular quantum chemistry contained in the Q-chem 4 program package. Mol Phys. 2015;113(2):184–215.
65. Kossoski F, Barbatti M. Nuclear ensemble approach with importance sampling. J Chem Theory Comput. 2018;14(6):3173–83.
66. Klaffki N, Weingart O, Garavelli M, Spohr E. Sampling excited state dynamics: influence of HOOP mode excitations in a retinal model. Phys Chem Chem Phys. 2012;14:142991430.
67. Barbatti M, Sen K. Effects of different initial condition samplings on photodynamics and spectrum of pyrrole. Int J Quantum Chem. 2016;116:762771.
68. Ceriotti M, Bussi G, Parrinello M. Langevin equation with colored noise for constant- temperature molecular dynamics simulations. Phys Rev Lett. 2009;102:020601. https://doi.org/10.1103/PhysRevLett.102.020601
69. Ceriotti M, Bussi G, Parrinello M. Colored-noise thermostats Ã la carte. J Chem Theory Comput. 2010;6(4):1170–80. https://doi.org/10.1021/ct900563s
70. Prlj A, Hollas D, Curchod BFE. Deciphering the influence of ground-state distributions on the calculation of photolysis observables. J Phys Chem A. 2023;127(35):7400–9. https://doi.org/10.1021/acs.jpca.3c02333
71. Clark LB, Peschel GG, Tinoco I. Vapor spectra and heats of vaporization of some purine and pyrimidine Bases1. J Phys Chem. 1965;69(10):3615–8. https://doi.org/10.1021/j100894a063
72. Barbatti M. Nonadiabatic dynamics with trajectory surface hopping method. WIREs Comput Mol Sci. 2011;1(4):620–33.
73. Richter M, Marquetand P, González-Vázquez J, Sola I, González L. SHARC: ab initio molecular dynamics with surface hopping in the adiabatic representation including arbitrary couplings. J Chem Theory Comput. 2011;7(5):1253–8.
74. Subotnik JE, Jain A, Landry B, Petit A, Ouyang W, Bellonzi N. Understanding the surface hopping view of electronic transitions and decoherence. Annu Rev Phys Chem. 2016;67:387–417.
75. Mai S, Marquetand P, González L. Surface hopping molecular dynamics. Quantum Chemistry and Dynamics of Excited States: Methods and Applications. Hoboken, NJ: John Wiley & Sons, Inc. 2020. p. 499–530.
76. Jain A, Sindhu A. Pedagogical overview of the fewest switches surface hopping method. ACS Omega. 2022;7(50):45810–24.
77. Tully JC. Molecular dynamics with electronic transitions. J Chem Phys. 1990;93(2):1061–71. https://doi.org/10.1063/1.459170
78. Meyer HD, Manthe U, Cederbaum LS. The multi-configurational time-dependent Hartree approach. Chem Phys Lett. 1990;165(1):73–8.
79. Dral PO, Barbatti M, Thiel W. Nonadiabatic excited-state dynamics with machine learning. J Phys Chem Lett. 2018;9(19):5660–3.
80. Westermayr J, Gastegger M, Menger MFSJ, Mai S, González L, Marquetand P. Machine learning enables long time scale molecular photodynamics simulations. Chem Sci. 2019;10:8100–7. https://doi.org/10.1039/C9SC01742A
81. Westermayr J, Marquetand P. Machine learning for electronically excited states of molecules. Chem Rev. 2020;121:9873–926.
82. Richings GW, Habershon S. Predicting molecular photochemistry using machine-learning-enhanced quantum dynamics simulations. Acc Chem Res. 2022;55(2):209–20.
83. Westermayr J, Gastegger M, Vörös D, Panzenboeck L, Joerg F, González L, et al. Deep learning study of tyrosine reveals that roaming can lead to photodamage. Nat Chem. 2022;14(8):914–9.
84. Zhu C, Nangia S, Jasper AW, Truhlar DG. Coherent switching with decay of mixing: an improved treatment of electronic coherence for non-born–Oppenheimer trajectories. J Chem Phys. 2004;121(16):7658–70.
85. Zhu C, Jasper AW, Truhlar DG. Non-born-Oppenheimer Liouville-von Neumann dynamics. Evolution of a subsystem controlled by linear and population-driven decay of mixing with decoherent and coherent switching. J Chem Theory Comput. 2005;1(4):527–40.
86. Granucci G, Persico M. Critical appraisal of the fewest switches algorithm for surface hopping. J Chem Phys. 2007;126(13):134114. https://doi.org/10.1063/1.2715585
87. Jain A, Alguire E, Subotnik JE. An efficient, augmented surface hopping algorithm that includes decoherence for use in large-scale simulations. J Chem Theory and Comput. 2016;12(11):5256–68.
88. Subotnik JE, Jain A, Landry B, Petit A, Ouyang W, Bellonzi N. Understanding the surface hopping view of electronic transitions and decoherence. Ann Rev Phys Chem. 2016;67(1):387–417.
89. Jaeger HM, Fischer S, Prezhdo OV. Decoherence-induced surface hopping. J Chem Phys. 2012;137(22):22A545. https://doi.org/10.1063/1.4757100
90. Akimov AV, Prezhdo OV. Advanced capabilities of the PYXAID program: integration schemes, decoherence effects, multiexcitonic states, and field-matter interaction. J Chem Theory Comput. 2014;10(2):789–804.
91. Schwartz BJ, Rossky PJ. Aqueous solvation dynamics with a quantum mechanical solute: computer simulation studies of the photoexcited hydrated electron. J Chem Phys. 1994;101(8):6902–16.
92. Nelson T, Fernandez-Alberti S, Roitberg AE, Tretiak S. Nonadiabatic excited-state molecular dynamics: treatment of electronic decoherence. J Chem Phys. 2013;138(22):224111.

93. Vindel-Zandbergen P, Ibele LM, Ha JK, Min SK, Curchod BFE, Maitra NT. Study of the decoherence correction derived from the exact factorization approach for nonadiabatic dynamics. J Chem Theory Comput. 2021;17(7):3852–62. https://doi.org/10.1021/acs.jctc.1c00346
94. Vindel-Zandbergen P, Matsika S, Maitra NT. Exact-factorization-based surface hopping for multistate dynamics. J Phys Chem Lett. 2022;13(7):1785–90. https://doi.org/10.1021/acs.jpclett.1c04132
95. Richter M, Marquetand P, González-Vázquez J, Sola I, González L. Correction to "SHARC–ab initio molecular dynamics with surface hopping in the adiabatic representation including arbitrary couplings" [J. Chem. Theory Comput 2011, 7, 1253–1258]. J Chem Theory Comput. 2012;8(1):374.
96. Mai S, Marquetand P, González L. Nonadiabatic dynamics: the SHARC approach. WIREs Comput Mol Sci. 2018;8(6):e1370. https://doi.org/10.1002/wcms.1370
97. Barbatti M, Ruckenbauer M, Plasser F, Pittner J, Granucci G, Persico M, et al. Newton-X: a surface-hopping program for nonadiabatic molecular dynamics. WIREs Comput Mol Sci. 2014;4(1):26–33. https://doi.org/10.1002/wcms.1158
98. Barbatti M, Bondanza M, Crespo-Otero R, Demoulin B, Dral PO, Granucci G, et al. Newton-X platform: new software developments for surface hopping and nuclear ensembles. J Chem Theory Comput. 2022;18(11):6851–65.
99. Mai S, Avagliano D, Heindl M, Marquetand P, Menger MFSJ, Oppel M, et al. SHARC3.0: surface hopping including arbitrary couplings. 2023 Program Package for Non-Adiabatic Dynamics; https://sharc-md.org/
100. Du L, Lan Z. An on-the-fly surface-hopping program jade for nonadiabatic molecular dynamics of polyatomic systems: implementation and applications. J Chem Theory Comput. 2015;11(4):1360–74.
101. Akimov AV, Prezhdo OV. The PYXAID program for non-adiabatic molecular dynamics in condensed matter systems. J Chem Theory Comput. 2013;9(11):4959–72.
102. Akimov AV. Libra: an open-source "methodology discovery" library for quantum and classical dynamics simulations. J Comput Chem. 2016;37:1626–49.
103. Shu Y, Zhang L, Truhlar DG. ANT 2023: a program for adiabatic and nonadiabatic trajectories. Comput Phys Commun. 2024;296:109021.
104. Ben-Nun M, Quenneville J, Martínez TJ. Ab initio multiple spawning: photochemistry from first principles quantum molecular dynamics. J Phys Chem A. 2000;104(22):5161–75.
105. Liu Y, Chakraborty P, Matsika S, Weinacht T. Excited state dynamics ofcis,cis-1,3-cyclooctadiene: UV pump VUV probe time-resolved photoelectron spectroscopy. J Chem Phys. 2020;153(7):074301.
106. Ortiz JV. Dyson-orbital concepts for description of electrons in molecules. J Chem Phys. 2020;153:070902.
107. Krylov AI. From orbitals to observables and back. J Chem Phys. 2020;153:080901.
108. Hudock HR, Levine BG, Thompson AL, Satzger H, Townsend D, Gador N, et al. Ab initio molecular dynamics and time-resolved photoelectron spectroscopy of electronically excited uracil and thymine. J Phys Chem A. 2007;111(34):8500–8.
109. Ponzi A, Angeli C, Cimiraglia R, Coriani S, Decleva P. Dynamical photoionization observables of the CS molecule: the role of electron correlation. J Chem Phys. 2014;140:204304.
110. Ruckenbauer M, Mai S, Marquetand P, González L. Revealing deactivation pathways hidden in time-resolved photoelectron spectra. Sci Rep. 2016;6:35522.
111. Chakraborty P, Liu Y, Weinacht T, Matsika S. Excited state dynamics of cis,cis-1,3-cyclooctadiene: non-adiabatic trajectory surface hopping. J Chem Phys. 2020;152(17):174302. https://doi.org/10.1063/5.0005558
112. Anstöter CS, Verlet JRR. Modeling the photoelectron angular distributions of molecular anions: roles of the basis set, orbital choice, and geometry. J Phys Chem A. 2021;125(22):4888–95. https://doi.org/10.1021/acs.jpca.1c03379
113. Hudock HR, Martínez TJ. Excited-state dynamics of cytosine reveal multiple intrinsic subpicosecond pathways. ChemPhysChem. 2008;9(17):2486–90.
114. Thompson AL, Martínez TJ. Time-resolved photoelectron spectroscopy from first principles: excited state dynamics of benzene. Faraday Discuss. 2011;150:293–311. https://doi.org/10.1039/C1FD00003A
115. Kuhlman TS, Glover WJ, Mori T, Møller KB, Martínez TJ. Between ethylene and polyenes - the non-adiabatic dynamics of cis-dienes. Faraday Discuss. 2012;157:193–212. https://doi.org/10.1039/C2FD20055D
116. MacDonell RJ, Schalk O, Geng T, Thomas RD, Feifel R, Hansson T, et al. Excited state dynamics of acrylonitrile: substituent effects at conical intersections interrogated via timeresolved photoelectron spectroscopy and ab initio simulation. J Chem Phys. 2016;145(11):114306.
117. Boguslavskiy AE, Schalk O, Gador N, Glover WJ, Mori T, Schultz T, et al. Excited state non-adiabatic dynamics of the smallest polyene, trans 1, 3-butadiene. I. Time-resolved photoelectron-photoion coincidence spectroscopy. J Chem Phys. 2018;148(16):164302.
118. Schuurman MS, Stolow A. Dynamics at conical intersections. Annu Rev Phys Chem. 2018;69:427–50.
119. MacDonell RJ, Corrales ME, Boguslavskiy AE, Bañares L, Stolow A, Schuurman MS. Substituent effects on nonadiabatic excited state dynamics: inertial, steric, and electronic effects in methylated butadienes. J Chem Phys. 2020;152(8):084308. https://doi.org/10.1063/1.5139446
120. Williams M, Forbes R, Weir H, Veyrinas K, MacDonell RJ, Boguslavskiy AE, et al. Unmasking the cis-stilbene phantom state via vacuum ultraviolet time-resolved photoelectron spectroscopy and ab initio multiple spawning. J Phys Chem Lett. 2021;12(27):6363–9. https://doi.org/10.1021/acs.jpclett.1c01227

121. Ruckenbauer M, Mai S, Marquetand P, González L. Revealing deactivation pathways hidden in time-resolved photoelectron spectra. Sci Rep. 2016;6:35522.
122. Chakraborty P. Investigating ultrafast photoexcited dynamics of organic chromophores. Temple University. Libraries 2020.
123. Chakraborty P, Liu Y, McClung S, Weinacht T, Matsika S. Nonadiabatic excited state dynamics of organic chromophores: take-home messages. J Phys Chem A. 2022;126(36):6021–31. https://doi.org/10.1021/acs.jpca.2c04671

How to cite this article: Chakraborty P, Matsika S. Time-resolved photoelectron spectroscopy via trajectory surface hopping. WIREs Comput Mol Sci. 2024;14(3):e1715. https://doi.org/10.1002/wcms.1715